2-15-2016

A High-Resolution Mid-Pleistocene Temperature Record from Arctic Lake El'gygytgyn: A 50 kyr Super Interglacial from MIS 33 to MIS 31?

Gregory De Wet
University of Massachusetts Amherst, gdewet@smith.edu

Isla S. Castañeda
University of Massachusetts Amherst

Robert M. DeConto
University of Massachusetts Amherst

Julie Brigham-Grette
University of Massachusetts Amherst

A high resolution mid-Pleistocene temperature record from Arctic Lake El'gygytgyn; a 50 kyr super interglacial from MIS 33-31?

Authors: Gregory de Wet [a *], Isla S. Castañeda [a], Robert M. DeConto [a], Julie Brigham-Grette [a]

[a] *Department of Geosciences, University of Massachusetts Amherst, Amherst, MA 01003 USA*

* Corresponding author. Tel: +1 717 725 2604.
Email address: gdewet@geo.umass.edu (G. de Wet)

Keywords: paleoclimatology; Arctic; Marine Isotope Stage 31; Super Interglacial; branched GDGT

1. Introduction

Placing predicted future climate change into a broader context necessitates detailed paleoclimate reconstructions that extend beyond the last glacial period, especially from high latitudes where such changes are expected to be the largest (Stocker et al., 2013). The term "super interglacial" has been used to describe periods in the past that appear to have been characterized by exceptionally warm conditions (DeConto et al., 2012; Melles et al., 2012; Pollard and DeConto, 2009), and as such are of great interest when searching for analogues of future climate. One such period is Marine Isotope Stage (MIS) 31, defined as 1.082-1.062 million years before present (Ma BP) by Lisiecki and Raymo (2005) (NB: in this study we refer to MIS boundaries as defined by the LR04 stack). Paleoclimate records from this period are desirable because MIS 31 falls beyond the current temporal range of the Antarctic ice cores, yet occurred during the Pleistocene, when the climate system and oceanographic gateways were generally similar to today.

MIS 31 was characterized by the highest summer insolation receipts at high latitudes of the past 1.2 Ma (Laskar et al., 2004), as well as some of the lowest oxygen isotopic values in the composite LR04 benthic stack (Lisiecki and Raymo, 2005). It has been identified as a period of extreme warmth in the southern high latitudes (e.g. Maiorano et al., 2009; Teitler et al., 2015) and is also the last time strong proxy evidence is available for a collapse of the West Antarctic Ice Sheet (WAIS) (McKay et al., 2012; Naish et al., 2009; Villa et al., 2012). In the Northern Hemisphere (NH), the vast majority of paleoclimate reconstructions that cover this period are marine sediment records, with notable exceptions being sediments from Lake Baikal (Khursevich et al., 2005) and the Chinese loess archives (Sun et al., 2010). However, no high-resolution terrestrial paleotemperature reconstructions from MIS 31 currently exist.

Here we present data from the Lake El'gygytgyn (northeast Russia) sediment record, which provides continuous coverage of MIS 31 (Melles et al., 2012). Our high-resolution brGDGT-based paleotemperature reconstruction spans MIS 33-31 (~1114 – 1050 kyr BP) at a time step of approximately 500 years. We find that MIS 31 in the Arctic experienced some of the warmest temperatures of the Pleistocene, but that peak warmth occurred out of phase with local summer insolation. Additionally, it appears that glacial conditions preceding this interval, during glacial stage 32, were short-lived in the

Arctic. This finding partially echoes recent evidence from the Southern Hemisphere (Teitler et al., 2015), where it was suggested that MIS 32 was warm at southern high latitudes and should be relegated to a stadial period instead of a glacial stage. The global signature of MIS 33-31 is discussed and potential teleconnections that could link changes in Antarctica and Lake El’gygytgyn are explored.

2. Site Description

The composite sediment core from Lake El’gygytgyn is exceptional in that it provides an archive of terrestrial paleoclimate covering the past 3.6 Ma (million years) from within the Arctic Circle (Figure 1) (Brigham-Grette et al., 2013). This site has already provided numerous insights into high latitude climate over the Plio-Pleistocene (Brigham-Grette et al., 2013; Melles et al., 2012; Climate of the Past Special Issue: Initial results from lake El'gygytgyn, western Beringia: first time-continuous Pliocene-Pleistocene terrestrial record from the Arctic), and MIS 31 has been identified as one of over a dozen “super interglacials” within this record. Warm conditions during this interval have been identified in other proxy reconstructions from Lake El’gygytgyn, such as pollen-based paleotemperatures, total organic carbon and biogenic silica concentrations, and elemental ratios (Melles et al., 2012).

Lake El’gygytgyn is located approximately 100 km north of the Arctic Circle in northeastern Siberia (67.5°N, 172°E) (Figure 1) and was created 3.58±0.25 Ma by a meteorite impact (Layer, 2000). The lake has a diameter of 12 km, with a total surface area of 110 km^2, and is 170 m deep. Today, the continental Arctic climate leads to tundra vegetation occupying the surrounding catchment and ice cover on the lake for 10 months of the year (Nolan and Brigham-Grette, 2007). The lake is classified as oligotrophic to ultra-oligotrophic, with full overturning occurring during the summer leading to an oxygenated water column throughout the year (Melles et al., 2012; Nolan and Brigham-Grette, 2007). Measurements from a thermistor string deployed in the lake indicates water temperatures vary from 0-4°C (Nolan and Brigham-Grette, 2007). Measured air temperatures at the lake over the calendar year 2002 indicate a mean annual air temperature (MAAT) of -10.3°C, with a maximum temperature of 26°C and a minimum of -40°C.

Average temperatures in July were ~10°C, which was shown to be representative of the broader region (Nolan and Brigham-Grette, 2007).

The lake was drilled during the winter of 2008/2009, resulting in a composite sediment sequence of ~320 m. The age model for the core is based primarily on magnetostratigraphy and tuning of paleo-productivity proxies to the benthic oxygen isotope stack and insolation curves (Haltia and Nowaczyk, 2014; Nowaczyk et al., 2013). Age uncertainty during the MIS 31 section of the core is, therefore, related to uncertainties in the LR04 stack (estimated to be up to 6 kyr from 1 to 3 Ma), but Nowaczyk et al. (2013) note that "relative age assignments to the reference records should have a precision of ~500 yr since many (3rd order) tie points were derived from the insolation reference record, which has a higher temporal resolution". Identification of MIS 31 in the composite sequence is aided by the presence of the Jaramillo paleomagnetic reversal (0.991-1.073 Ma) (Haltia and Nowaczyk, 2014). For further details the reader is referred to Nowaczyk et al. (2013). Sedimentation rates were relatively high during the Pliocene (~50 cm kyr^{-1}), and then decreased during the Pleistocene (~4-5 cm kyr^{-1}), with brief intervals of much higher sedimentation (Supplementary Materials) (Melles et al., 2012). During the MIS 35-29 study interval, the sedimentation rate varies from ~5-30 cm kyr^{-1} (Supplementary Materials). The MIS 31 section of the core spans approximately 100 cm.

3. Methods

For this study 143 sediment samples (~1-8 g dry mass) were taken spanning MIS 29-35 (approx. 1010-1145 kyr BP). The majority of samples from MIS 33-31 were taken at centimeter increments, resulting in a sample resolution of ~500 years per sample. The sediment was freeze-dried and homogenized using a mortar and pestle before lipid extraction.

A total lipid extract (TLE) was obtained using a Dionex accelerated solvent extractor (ASE 200). Samples were extracted with a dichloromethane (DCM)/methanol (9:1, v/v) mixture at 100°C. The TLE was then separated into two fractions, apolar (9:1 DCM:hexane, v/v) and polar (1:1 DCM:methanol), using alumina oxide column chromatography. Polar fractions were filtered in 99:1 hexane:isopropanol using a 0.45µm PTFE syringe filter. A C_{46} GDGT internal standard was added to all polar fractions prior to analysis.

BrGDGTs were identified and quantified via high performance liquid chromatography - mass spectrometry using an Agilent 1260 HPLC coupled to an Agilent 6120 MSD following the methods of Hopmans et al. (2000) with minor modifications (Schouten et al., 2007). For compound separation a Prevail Cyano column (150 x 2.1mm, 3 µm) was used. Two solvent mixtures were used as eluents: mixture A) 100% hexane; mixture B) 90% hexane, 10% isopropanol (v/v). Samples were eluted with 10% mixture B for 5 minutes, which was then linearly increased to 18% mixture B from minutes 5-39, and finally increased to 100% mixture B for one minute. Scanning was performed in selected ion monitoring (SIM) mode. Concentrations were calculated by comparing brGDGT HPLC-MS chromatogram peak areas with peak areas of a known concentration (C_{46} GDGT standard added to every sample run). These values were then normalized to the mass of sediment extracted.

Further paleoenvironmental conditions were reconstructed using two indices based on brGDGT concentrations as originally defined by Weijers et al. (2007). The first is the cyclisation ratio of branched tetraethers (CBT) (Eq. 1). This index measures the relative amount of cyclopentyl moieties in the branched GDGTs, which Weijers et al. (2007) found to be correlated to pH. The second index, the Methylation of Branched Tetraethers (MBT), measures the presence of methyl branches at the C-5 and C-5’ positions and was found to be positively correlated to MAAT, and to a lesser extent, negatively correlated to pH (Eq. 2). By combining these two indices, Weijers et al. (2007) were able to produce a robust paleotemperature proxy for soil-derived brGDGTs. In recent years this MBT/CBT relationship has been expanded to include lake sediment samples, yielding numerous lake specific calibrations (e.g. (Loomis et al., 2012; Pearson et al., 2011; Sun et al., 2011; Tierney et al., 2010). For this study the calibration of Sun et al. (2011) (Eq. 3) was applied to reconstruct temperature. In equations 1 and 2 the roman numerals and letters denote the different brGDGT structures as shown in Figure A1, Appendix A in Weijers et al. (2007).

Eq. 1: **CBT** = $\frac{[\mathbf{Ib}]+[\mathbf{IIb}]}{[\mathbf{I}]+[\mathbf{II}]}$ (Weijers et al., 2007)

Eq. 2: **MBT** = $\frac{[\mathbf{I+Ib+Ic}]}{[\mathbf{I+Ib+Ic}]+[\mathbf{II+IIb+IIc}]+[\mathbf{III+IIIb+IIIc}]}$ (Weijers et al., 2007)

Eq. 3: $\boldsymbol{T = 6.803 - 7.602\ \times CBT + 37.090\ \times MBT}$ (Sun et al., 2011)

4. Results

Branched GDGT results from this study are plotted in Figure 2. brGDGTs are present in all samples analyzed in this study. Total brGDGT concentrations vary from 0.0039 µg/g sediment to 1.039 µg/g sediment, with a mean concentration of 0.23 µg/g sediment. Generally, concentrations are higher during inferred interglacial periods, with the notable exception of ~1100-1110 kyr BP, when the highest concentrations of the studied interval occur briefly during glacial MIS 32. Values for the MBT Index range from 0.075 to 0.36, with a mean of 0.22. The CBT Index ranges from 0.084 to 1.37 with a mean of 0.48.

Reconstructed temperatures based on the MBT/CBT index vary from between 17.3 and 4.0^{o}C, with a mean value of 11.8^{o}C using the calibration of Sun et al. (2011). Twenty eight samples were run in duplicate, with a standard error of 0.1^{o}C. Temperatures rise from 6-8^{o}C during MIS 34 to ~14-17^{o}C during MIS 33 (Figure 2). Temperatures then decrease relatively rapidly to between 4 and 8^{o}C at the start of MIS 32. This cooling is short-lived, however, with temperatures rising to ~13^{o}C after only a few thousand years. Temperatures remain generally warm but variable until ~1088 kyr BP, when an increase of 4.5^{o}C is observed. This extreme warmth during MIS 32, reaching 17.5^{o}C, is supported by 4 samples representing ~2,000 years. Temperatures then rapidly decrease back to around 13^{o}C. They slowly rise during the traditional definition of the beginning of MIS 31 to ~16^{o}C before declining into glacial MIS

30, punctuated by numerous episodes of abrupt temperature change (4-5^{o}C over less than a thousand years).

Reconstructed pH using the calibration of Sun et al. (2011) yields a maximum of 8.8 and a minimum pH of 7.3 (mean of 8.2). While reconstructed pH does generally seem to covary with reconstructed temperature, there are periods when large changes in pH are not accompanied by a major temperature change (e.g. ~1093-1092 kyr BP) and vice versa (1108-1107 kyr BP) (Figure 2).

5. Discussion

5.1 brGDGT temperature reconstruction

Our paleotemperature reconstructions are based on concentrations of brGDGTs extracted from sediments. These compounds are bacterial membrane lipids that differ in the number of methyl branches and cyclopentane groups in their structures (Hopmans et al., 2004). The distribution of these methyl branches and cyclopentyl moieties was originally shown to be related to temperature and, to a lesser extent, pH, in soils and peat (Weijers et al., 2007). This relationship has since been observed in lake sediments as well, with increasing evidence for autochthonous production of brGDGTs in the water column (e.g. Loomis et al., 2014; Tierney et al., 2010). Modern calibration studies are used to derive pH and air temperature estimates from brGDGT distributions back through time (e.g (Loomis et al., 2012; Pearson et al., 2011; Tierney et al., 2010).

In this study, temperature reconstructions using the CBT and MBT indices were calculated based on the calibration of Sun et al. (2011) (Eq. 3). This decision was based mainly on the fact that this calibration is in agreement with reconstructed mean temperature of the warmest month (MTWM) estimates from pollen data over the same interval (purple line, Figure 3). It also incorporates lake-derived data from China and Nepal, the spatially closest sites to Lake El'gygytgyn. We note that applying other lake-specific MBT/CBT calibrations (e.g Loomis et al., 2012; Tierney et al., 2010; Yang et al., 2014) produces a wide range of absolute temperatures (differences of up to 6^{o}C for the same sample). However, relative temperature changes are similar regardless of which MBT/CBT calibration is applied. We have also applied brGDGT fractional abundance calibrations (e.g. Loomis et al., 2012; Pearson et al., 2011; Tierney et al., 2010), but those resulted in numerous unrealistic (>30°C) temperatures at certain periods in the record. We also note recent research suggesting the dependence of MBT on pH is related to incomplete separation of 6-methyl isomers on all penta- and hexa-methylated brGDGTs using current methods (De Jonge et al., 2014, 2013). While we are aware of this new methodology to separate these isomers, the majority of our analyses were carried out prior to the publication of this method.

We suggest that the majority of brGDGTs that have accumulated in Lake El'gygytgyn sediments were not sourced from catchment soils and likely come from *in-situ* production in the water column. While we cannot entirely rule out production in the sediments themselves, numerous studies have shown that the majority of brGDGTs are being produced in the upper water column (e.g. Buckles et al., 2014; Loomis et al., 2014). Because the catchment of Lake El'gygytgyn is roughly circular and bounded by the crater walls formed from the meteorite impact, the basin (15km in diameter) drains a small area relative to the size of the lake (12km in diameter). The lake is also surrounded by continuous permafrost (Nolan and Brigham-Grette, 2007), and a preliminary analysis of a soil core collected from within the catchment was essentially bereft of brGDGTs (Bischoff, pers. comm. 2014). Additionally the bottom water temperature of Lake El'gygytgyn remains a nearly constant 4°C throughout the year (Nolan and Brigham-Grette, 2007), inconsistent with the large variations seen in MBT values and reconstructed temperature.

We also assume that our reconstruction represents summer temperature. Studies from mid to high latitude lakes have noted the strongest relationship between brGDGT indicies and summer/warm months temperature (Pearson et al., 2011; Shanahan et al., 2013; Sun et al., 2011). Shanahan et al. (2013) note that this warm season bias is likely due to increased biological productivity during the summer months (higher temperatures, lakes are ice-free, greatest number of daylight hours). Lake El'gygytgyn is currently only ice free for approximately two months during July and August (Nolan and Brigham-Grette, 2007), and it is likely that the majority of primary production at/in the lake occurs during this period. Mean summer temperatures at the lake today are ~10°C, which compares favorably with our reconstructions based on the Sun et al. (2011) calibration (Figure 3). We note, however, that without a site-specific calibration, or at least more knowledge of local sources of GDGT production, absolute temperature reconstructions using any external calibration should be regarded with caution. In spite of this uncertainty, we expect relative temperature changes reconstructed using the MBT/CBT proxy to be robust, as supported by temperature reconstructions from pollen assemblage data, and these changes form the basis for the majority of our conclusions.

5.2 Super Interglacial MIS 31 at Lake El'gygytgyn

While we hesitate to draw conclusions on the absolute temperature values reached during the studied interval due to the calibration issues mentioned above, numerous interesting features are apparent based on relative temperature changes. The first is the apparent warm nature of glacial MIS 32 at Lake El'gygytgyn (Figure 3). Average brGDGT based temperatures for MIS 33-31 are shown in Table 1. Mean temperatures during MIS 32 (1081-1104 kyr) are only ~0.5^{o}C lower than MIS 31, and only 0.1^{o}C lower than MIS 33 (similar regardless of MBT/CBT calibration chosen). Cold conditions are recorded only briefly for ~2 kyr centered around 1102 kyr BP (Figure 3). This warming pattern shows a dramatic departure from both boreal summer insolation and the LR04 stack, suggesting that other factors were influencing climate at Lake El'gygytgyn during this time.

Table 1: Average reconstructed temperatures from MIS 33-31

Marine Isotope Stage	Average MBT/CBT Temperature (^{o}C)	Minimum Temperature (^{o}C)	Maximum Temperature (^{o}C)
31	12.8	8.6	16.0
32	12.2	5.6	17.3
33	12.3	11.6	17.2

Other published proxies from the lake provide limited insight on this observation (Figure 3) (Melles et al., 2012). Mean temperature of the warmest month (MTWM) estimates based on pollen reconstructions, which agree well with our brGDGT data during most of MIS 31, deviate in the early part of MIS 31/late 32 (where only 3 data points exist). The % of tree and shrub pollen in the lake shows a dramatic increase between 1091.5 kyr and 1086 kyr BP, well before peak NH insolation, but low sample resolution, along with the potential influence of precipitation on vegetation, precludes robust conclusions. The accumulation of biogenic silica (based on Si/Ti ratios) steadily increases from a minima ~1101 kyr BP (the same time the lowest brGDGT temperatures for MIS 32 are recorded) to a maximum ~1072 kyr BP. While it does not display the dramatic fluctuations seen in the MBT/CBT data, it does appear that the low productivity seen around 1100 kyr BP was short lived during MIS 32. Perhaps most notable is the presence of the characteristic "super interglacial" sediment facies during MIS 32 at Lake El'gygytgyn (Melles et al., 2012) (Figure 3), suggesting extremely warm conditions at the lake prior to the traditional definition for the onset of MIS 31.

Also worth noting is the presence of abrupt episodes of both warming and cooling throughout the high-resolution section of our record. Perhaps most notable is the relatively abrupt warming event just prior to the onset of MIS 31 (ca. 1087-1084 kyr BP), which is defined by multiple data points. This event is close in timing to a small peak noted in the global benthic $\delta^{18}O$ record within the MIS 31 interval (Figure 4) and considering uncertainties in both age models, may be coincident. While this event has not yet been resolved in other marine or terrestrial records lacking the resolution of the Lake El'gygytgyn core, it may have been global, given similarities in timing to the excursion in the benthic $\delta^{18}O$ record.

In summary, our record demonstrates considerable high-frequency variability in temperature during this time interval. It also suggests that the entire period encompassing MIS 33-31 was generally warm in the Arctic. Existing proxies from Lake El'gygytgyn either suggest that warm conditions prevailed at the lake prior to the traditional definition of MIS 31, or are of insufficient resolution to rule out this possibility. Further analyses, including higher resolution pollen sampling and the determination of the deuterium isotopic composition of leaf waxes, will help confirm this assertion.

5.3 Global Signature of MIS 33-31

The observation that Lake El'gygytgyn appears warm during MIS 32 echoes recent findings from high southern latitudes (Teitler et al., 2015), where the majority of research pertaining to MIS 31 explicitly has been carried out to date (DeConto et al., 2012; Maiorano et al., 2009; McKay et al., 2012; Villa et al., 2012, 2008). Results from the ANDRILL project (McKay et al., 2012; Naish et al., 2009; Scherer et al., 2008; Villa et al., 2012) noted the presence of diatomite and presumed open water conditions at the coring site in the Ross Sea (Figure 1), implying a dramatically reduced West Antarctic Ice Sheet (WAIS) during this time. A large-scale reduction in WAIS is further supported by the modeling studies of Pollard and DeConto (2009) and DeConto et al. (2012). The authors also found reduced sea ice concentrations around the entire continent. Elsewhere around the Antarctic margin, Villa et al. (2008) found evidence for a major shift in dominant circulation patterns in the form of a decrease or disappearance of the Polar Front (indicated by increases in warm water nannofossil assemblages) at Sites 1165 and 1167 (Prydz Bay, East Antarctica) (Figure 1). This finding was echoed further from the Antarctic continent, with evidence for a southward migration of the Subtropical Front at Site 1090 (Maiorano et al., 2009) (Figure 1).

Although MIS 31 has been identified as an exceptional event in the SH, the exact timing of warmth is still a subject of debate. The majority of the studies mentioned above ascribed peak interglacial conditions to ~1080 kyr BP, when austral summer insolation was at a maximum (~10 kyr earlier than the boreal summer insolation peak during MIS 31 ~1070 kyr) (Figure 4). However, a recent study by Teitler et al. (2015) revisited the age models of the ANDRILL, CRP-1 (Cape Roberts), Site 1165 and Site 1090 records and concluded that a secondary interpretation may be that warm conditions actually began earlier, during MIS 33. The authors also analyzed iceberg rafted detritus (IRD) and found minimal accumulation of IRD across the entirety of MIS 33-31 at Site 1090 (Teitler et al., 2015). The timing of the decrease in IRD agrees strongly with our reconstructed warm temperatures at Lake El'gygytgyn (Figure 4). In summary, Teitler et al. (2015) suggest that glacial MIS 32 be relegated from a glacial stage to a stadial and that MIS 31 be reclassified as a longer interglacial more akin to later post Mid-Pleistocene Transition interglacials, lasting closer to 50 kyr BP instead of the ~20 kyr as it is currently defined. The authors point to another SH austral insolation peak at the beginning of MIS 33 as the potential catalyst for the beginning of this long interglacial.

The apparent strong linkage between Lake El'gygytgyn and records from the Antarctic margin has been highlighted previously (Melles et al., 2012; Brigham-Grette et al. 2013). The authors suggest that dramatic warming in the SH (reduction of WAIS, less sea ice) would lead to reduced Antarctic Bottom Water (AABW) production during this time (e.g. McKay et al., 2012). Less AABW production could lead to decreased northward flow of deep water into the North Pacific, subsequently reducing upwelling and increasing water column stratification (Melles et al., 2012). The resulting increase in sea surface temperature might then lead to changes in air temperature at Lake El'gygytgyn, although this has not been supported by modeling efforts to date (Melles et al., 2012). Possible evidence for this mechanism operating during MIS 31 comes in the form of lower concentrations of sortable silt off the coast of New Zealand (Hall et al., 2001) as well as low rates of biogenic silica accumulation at Site 882 in the North Pacific (Haug et al., 1999) (Figure 1).

Previously this reduction of AABW and subsequent changes in ocean circulation has been suggested as a mechanism for the warmth of MIS 31 proper. However, existing proxy records have not been of sufficient resolution to investigate more intricate timing and relationships with insolation or other global climate records such as the benthic oxygen isotope stack (Lisiecki and Raymo, 2005). In light of our temperature reconstruction, however, it could be interpreted as a mechanism that can explain the warmth during MIS 32 (when SH insolation was high, prior the NH peak) (Figure 4). A recent study by Hao et al. (2015) also pointed to changes in Antarctic ice volume driving prolonged interglacial conditions in the NH during MIS 15-13. More research is required to substantiate this interhemispheric linkage, but it does provide a plausible explanation for the apparent connection between SH records and the warming seen in western Beringia.

Looking beyond the poles, paleotemperature reconstructions that cover this period in sufficient resolution to be meaningful are generally limited to sea surface temperature (SST) records (Figure 5). While a limited number of terrestrial archives do span MIS 31, existing data are mainly limited to indirect climate proxies: biogenic silica from Lake Baikal (Khursevich et al., 2005), magnetic susceptibility and grain size from Chinese loess (Sun et al., 2010). However, these proxies more closely track local summer insolation values. Of the SST data plotted here, the majority are part of longer time-series, and as such have not been interpreted in relation to MIS 31 specifically. Interestingly, however, the majority of data suggest that MIS 32 was either reduced in duration or magnitude, similar to our Lake El'gygytgyn data. The upper part of Figure 5 (Sites 722-1123) depicts SST records where MIS 32 appears to be a relatively "weak" glacial compared to other cold periods. Cooling within the shaded area (MIS 33-31) does not seem to reach the low temperatures of MIS 34 or 30, for example. The lower section of Figure 5 (Sites 882-1090) alternatively suggests that although cooling may have reached a similar magnitude as other mid-Pleistocene glacial periods, the duration appears abbreviated (only a few kyr). Closer analysis of the LR04 benthic stack also indicates that MIS 32 was a weaker glacial period compared to 34 and 30. It also suggests, however, that at least some return to glacial conditions must have occurred (high $\delta^{18}O$ values around 1100 kyr BP).

More widely distributed high-resolution records are required to provide a definitive answer on the glacial versus stadial nature of MIS 32 globally. The highest resolution ocean SST records presented here have a resolution of 1-2 kyr (Herbert et al., 2010), and in many cases the "glacial" temperatures representing MIS 32 (Figure 5) are represented by only one or two data points. Alternatively other records spanning this interval may be missing the coldest periods of MIS 32. However, based on the available evidence from the Beringian Arctic, high southern latitudes, and existing SST records, it seems that MIS 32 was reduced in magnitude and/or duration relative to other glacial intervals of the Pleistocene.

The underlying cause of the protracted warmth around MIS 31 remains elusive. The unique nature of this super interglacial is thought to have occurred largely in response to summer insolation during this time (DeConto et al., 2012), which was anomalously high (especially at the poles) due to the concurrence of high obliquity and high eccentricity. Insolation values at 65°N in July for instance, were nearly 30 Wm^{-2} higher during peak MIS 31 than our current interglacial (Laskar et al., 2004). In the NH, however, peak boreal insolation occurs ~1070 kyr BP, significantly after peak temperatures are recorded at Lake El'gygytgyn (Figure 4). SH austral summer insolation is highest one half a precession cycle earlier (~1080 kyr BP), but again this is too late to explain the warming suggesting by Teitler et al. (2015), and our temperature record beginning at MIS 33 (~1114 kyr BP). In relation to our temperature reconstruction, it is plausible that the alternating insolation peaks between hemispheres, separated by half a precession cycle, could register as a continued period of warmth at Lake El'gygytgyn, through oceanic teleconnections linked to Antarctic ice volume. It seems unlikely, however, that insolation alone triggered a substantial WAIS retreat at the beginning of MIS 33 (when maximum austral insolation values reached only ~511 Wm^{-2} at the end of the interglacial (Laskar et al., 2004) (Figure 4).

While greenhouse gas concentrations likely played a role, their relative contribution remains unresolved. High concentrations of CO_2 have been explored as a possible forcing in model simulations during MIS 31 (DeConto et al., 2012), but current proxy reconstructions are of insufficient resolution and/or fidelity to be definitive. While there may be a relative peak in CO_2 concentrations in the reconstruction of Honisch et al. (2009) ~1 Ma BP it is only supported by 2-3 data points. Generally, existing CO_2 reconstructions do not suggest dramatically higher concentrations relative to other Pleistocene interglacials (Honisch et al., 2009; Tripati et al., 2011).

More research is needed to definitively characterize MIS 32 at Lake El'gygytgyn. Lower "glacial" temperatures are recorded during MIS 32 in our brGDGT data, albeit briefly, and the question of glacial stage versus stadial could change depending on whether duration or intensity is deemed more important. Extension of pollen analyses back to MIS 33 and planned deuterium istotopic analyses of leaf waxes will provide further independent reconstructions to compare to our brGDGT temperatures. More global high-resolution records will similarly be of great use in determining the true nature of this period.

Conclusions

BrGDGTs are present in the Lake El'gygytgyn sediment record throughout the interval surrounding MIS 31, and reconstructed temperatures are in agreement with pollen based summer temperature estimates from the same interval. While we acknowledge the absolute reconstructed temperatures using this methodology are reliant on the calibration chosen and should be treated with caution, relative temperature changes revealed by the brGDGT record nevertheless provides insight into the pattern of temperature variability, duration and intensity of super interglacial MIS 31 in the terrestrial Arctic. Our high-resolution reconstruction displays numerous abrupt temperature changes on the order of 4-6°C over a few thousand years or less. Additionally it appears that apart from a brief period ~1104 kyr BP, conditions at Lake El'gygytgyn were relatively warm during glacial Stage MIS 32. While this finding echoes recent results from the SH, more research is needed to determine whether the entire period of MIS 33-31 should be reclassified as one long interglacial. Should this prove true, it would add to the complexity surrounding the Mid-Pleistocene Transition.

Acknowledgements

We thank Jeff Salacup, Ben Keisling, and Helen Habicht for meaningful discussions and Jeff for his assistance in the laboratory. Juliane Bischoff is acknowledged for sharing insights on unpublished data. We thank two anonymous reviewers whose meaningful comments and suggestions improved the manuscript. Data associated with this study will be made available on the NOAA National Centers for Environmental Information website. Drilling operations at Lake El'gygtgyn were funded by the International Continental Scientific Drilling Program (ICDP), the US National Science Foundation (NSF), the German Federal Ministry of Education and Research (BMBF), Alfred Wegener Institute (AWI) and GeoForschungsZentrum Potsdam (GFZ), the Russian Academy of Sciences Far East Branch (RAS FEB), the Russian Foundation for Basic Research (RFBR), and the Austrian Federal Ministry of Science and Research (BMWF). Primary funding for this research was provided by NSF grant # 1204087.

References:

Brigham-Grette, J., Melles, M., Minyuk, P., Andreev, A., Tarasov, P., DeConto, R., Koenig, S., Nowaczyk, N., Wennrich, V., Rosen, P., Haltia, E., Cook, T., Gebhardt, C., Meyer-Jacob, C., Snyder, J., Herzschuh, U., 2013. Pliocene Warmth, Polar Amplification, and Stepped Pleistocene Cooling Recorded in NE Arctic Russia. Science 340, 1421–1427. doi:10.1126/science.1233137

Buckles, L.K., Weijers, J.W.H., Verschuren, D., Sinninghe Damsté, J.S., 2014. Sources of core and intact branched tetraether membrane lipids in the lacustrine environment: Anatomy of Lake Challa and its catchment, equatorial East Africa. Geochim. Cosmochim. Acta 140, 106–126. doi:10.1016/j.gca.2014.04.042

Crundwell, M., Scott, G., Naish, T., Carter, L., 2008. Glacial–interglacial ocean climate variability from planktonic foraminifera during the Mid-Pleistocene transition in the temperate Southwest Pacific, ODP Site 1123. Palaeogeogr. Palaeoclimatol. Palaeoecol. 260, 202–229. doi:10.1016/j.palaeo.2007.08.023

DeConto, R.M., Pollard, D., Kowalewski, D., 2012. Modeling Antarctic ice sheet and climate variations during Marine Isotope Stage 31. Glob. Planet. Change 88-89, 45–52. doi:10.1016/j.gloplacha.2012.03.003

De Jonge, C., Hopmans, E.C., Stadnitskaia, A., Rijpstra, W.I.C., Hofland, R., Tegelaar, E., Sinninghe Damsté, J.S., 2013. Identification of novel penta- and hexamethylated branched glycerol dialkyl glycerol tetraethers in peat using HPLC–MS2, GC–MS and GC–SMB-MS. Org. Geochem. 54, 78–82. doi:10.1016/j.orggeochem.2012.10.004

De Jonge, C., Hopmans, E.C., Zell, C.I., Kim, J.-H., Schouten, S., Sinninghe Damsté, J.S., 2014. Occurrence and abundance of 6-methyl branched glycerol dialkyl glycerol tetraethers in soils: Implications for palaeoclimate reconstruction. Geochim. Cosmochim. Acta 141, 97–112. doi:10.1016/j.gca.2014.06.013

Dyez, K.A., Ravelo, A.C., 2014. Dynamical changes in the tropical Pacific warm pool and zonal SST gradient during the Pleistocene: Tropical Pacific SST gradients. Geophys. Res. Lett. 41, 7626–7633. doi:10.1002/2014GL061639

Hall, I.R., McCave, I.N., Shackleton, N.J., Weedon, G.P., Harris, S.E., 2001. Intensified deep Pacific inflow and ventilation in Pleistocene glacial times. Nature 412, 809–812.

Haltia, E.M., Nowaczyk, N.R., 2014. Magnetostratigraphy of sediments from Lake El'gygytgyn ICDP Site 5011-1: paleomagnetic age constraints for the longest paleoclimate record from the continental Arctic. Clim. Past 10, 623–642. doi:10.5194/cp-10-623-2014

Hao, Q., Wang, L., Oldfield, F., Guo, Z., 2015. Extra-long interglacial in Northern Hemisphere during MISs 15-13 arising from limited extent of Arctic ice sheets in glacial MIS 14. Sci. Rep. 5, 12103. doi:10.1038/srep12103

Haug, G.H., Sigman, D.M., Tiedemann, R., Pedersen, T.F., Sarnthein, M., 1999. Onset of permanent stratification in the subarctic Pacific Ocean. Nature 401, 779–782.

Herbert, T.D., Peterson, L.C., Lawrence, K.T., Liu, Z., 2010. Tropical Ocean Temperatures Over the Past 3.5 Million Years. Science 328, 1530–1534. doi:10.1126/science.1185435

Honisch, B., Hemming, N.G., Archer, D., Siddall, M., McManus, J.F., 2009. Atmospheric Carbon Dioxide Concentration Across the Mid-Pleistocene Transition. Science 324, 1551–1554. doi:10.1126/science.1171477

Hopmans, E.C., Schouten, S., Pancost, R.D., van der Meer, M.T., Sinninghe Damsté, J.S., 2000. Analysis of intact tetraether lipids in archaeal cell material and sediments by high performance liquid chromatography/atmospheric pressure chemical ionization mass spectrometry. Rapid Commun. Mass Spectrom. 14, 585–589.

Hopmans, E.C., Weijers, J.W.., Schefuß, E., Herfort, L., Sinninghe Damsté, J.S., Schouten, S., 2004. A novel proxy for terrestrial organic matter in sediments based on branched and isoprenoid tetraether lipids. Earth Planet. Sci. Lett. 224, 107–116. doi:10.1016/j.epsl.2004.05.012

Khursevich, G.K., Prokopenko, A.A., Fedenya, S.A., Tkachenko, L.I., Williams, D.F., 2005. Diatom biostratigraphy of Lake Baikal during the past 1.25Ma: new results from BDP-96-2 and BDP-99 drill cores. Quat. Int. 136, 95–104. doi:10.1016/j.quaint.2004.11.011

Laskar, J., Robutel, P., Joutel, F., Gastineau, M., Correia, A.C.M., Levrard, B., others, 2004. A long-term numerical solution for the insolation quantities of the Earth. Astron. Astrophys. 428, 261–285.

Layer, P.W., 2000. Argon-40/argon-39 age of the El'gygytgyn impact event, Chukotka, Russia. Meteorit. Planet. Sci. 35, 591–599.

Li, L., Li, Q., Tian, J., Wang, P., Wang, H., Liu, Z., 2011. A 4-Ma record of thermal evolution in the tropical western Pacific and its implications on climate change. Earth Planet. Sci. Lett. 309, 10–20. doi:10.1016/j.epsl.2011.04.016

Lisiecki, L.E., Raymo, M.E., 2005. A Pliocene-Pleistocene stack of 57 globally distributed benthic $\delta^{18}O$ records: PLIOCENE-PLEISTOCENE BENTHIC STACK. Paleoceanography 20, n/a–n/a. doi:10.1029/2004PA001071

Loomis, S.E., Russell, J.M., Heureux, A.M., D'Andrea, W.J., Sinninghe Damsté, J.S., 2014. Seasonal variability of branched glycerol dialkyl glycerol tetraethers (brGDGTs) in a temperate lake system. Geochim. Cosmochim. Acta 144, 173–187. doi:10.1016/j.gca.2014.08.027

Loomis, S.E., Russell, J.M., Ladd, B., Street-Perrott, F.A., Sinninghe Damsté, J.S., 2012. Calibration and application of the branched GDGT temperature proxy on East African lake sediments. Earth Planet. Sci. Lett. 357-358, 277–288. doi:10.1016/j.epsl.2012.09.031

Maiorano, P., Marino, M., Flores, J.-A., 2009. The warm interglacial Marine Isotope Stage 31: Evidences from the calcareous nannofossil assemblages at Site 1090 (Southern Ocean). Mar. Micropaleontol. 71, 166–175. doi:10.1016/j.marmicro.2009.03.002

Martínez-Garcia, A., Rosell-Melé, A., McClymont, E.L., Gersonde, R., Haug, G.H., 2010. Subpolar link to the emergence of the modern equatorial Pacific cold tongue. Science 328, 1550–1553.

McClymont, E.L., Rosell-Melé, A., 2005. Links between the onset of modern Walker circulation and the mid-Pleistocene climate transition. Geology 33, 389. doi:10.1130/G21292.1

McClymont, E.L., Rosell-Melé, A., Giraudeau, J., Pierre, C., Lloyd, J.M., 2005. Alkenone and coccolith records of the mid-Pleistocene in the south-east Atlantic: Implications for the U37K′ index and South African climate. Quat. Sci. Rev. 24, 1559–1572. doi:10.1016/j.quascirev.2004.06.024

McKay, R., Naish, T., Powell, R., Barrett, P., Scherer, R., Talarico, F., Kyle, P., Monien, D., Kuhn, G., Jackolski, C., Williams, T., 2012. Pleistocene variability of Antarctic Ice Sheet extent in the Ross Embayment. Quat. Sci. Rev. 34, 93–112. doi:10.1016/j.quascirev.2011.12.012

Medina-Elizalde, M., Lea, D.W., Fantle, M.S., 2008. Implications of seawater Mg/Ca variability for Plio-Pleistocene tropical climate reconstruction. Earth Planet. Sci. Lett. 269, 585–595.

Melles, M., Brigham-Grette, J., Minyuk, P.S., Nowaczyk, N.R., Wennrich, V., DeConto, R.M., Anderson, P.M., Andreev, A.A., Coletti, A., Cook, T.L., Haltia-Hovi, E., Kukkonen, M., Lozhkin, A.V., Rosen, P., Tarasov, P., Vogel, H., Wagner, B., 2012a. 2.8 Million Years of Arctic Climate Change from Lake El'gygytgyn, NE Russia. Science 337, 315–320. doi:10.1126/science.1222135

Naafs, B.D.A., Hefter, J., Grützner, J., Stein, R., 2013. Warming of surface waters in the mid-latitude North Atlantic during Heinrich events: HIGH SSTs DURING HEINRICH EVENTS. Paleoceanography 28, 153–163. doi:10.1029/2012PA002354

Naish, T., Powell, R., Levy, R., Wilson, G., Scherer, R., Talarico, F., Krissek, L., Niessen, F., Pompilio, M., Wilson, T., Carter, L., DeConto, R., Huybers, P., McKay, R., Pollard, D., Ross, J., Winter, D., Barrett, P., Browne, G., Cody, R., Cowan, E., Crampton, J., Dunbar, G., Dunbar, N., Florindo, F., Gebhardt, C., Graham, I., Hannah, M., Hansaraj, D., Harwood, D., Helling, D., Henrys, S., Hinnov, L., Kuhn, G., Kyle, P., Läufer, A., Maffioli, P., Magens, D., Mandernack, K., McIntosh, W., Millan, C., Morin, R., Ohneiser, C., Paulsen, T., Persico, D., Raine, I., Reed, J., Riesselman, C., Sagnotti, L., Schmitt, D., Sjunneskog, C., Strong, P., Taviani, M., Vogel, S., Wilch, T., Williams, T., 2009. Obliquity-paced Pliocene West Antarctic ice sheet oscillations. Nature 458, 322–328. doi:10.1038/nature07867

Nolan, M., Brigham-Grette, J., 2007. Basic hydrology, limnology, and meteorology of modern Lake El’gygytgyn, Siberia. J. Paleolimnol. 37, 17–35. doi:10.1007/s10933-006-9020-y

Nowaczyk, N.R., Haltia, E.M., Ulbricht, D., Wennrich, V., Sauerbrey, M.A., Rosén, P., Vogel, H., Francke, A., Meyer-Jacob, C., Andreev, A.A., Lozhkin, A.V., 2013. Chronology of Lake El’gygytgyn sediments. Clim. Past Discuss. 9, 3061–3102. doi:10.5194/cpd-9-3061-2013

Pearson, E.J., Juggins, S., Talbot, H.M., Weckström, J., Rosén, P., Ryves, D.B., Roberts, S.J., Schmidt, R., 2011. A lacustrine GDGT-temperature calibration from the Scandinavian Arctic to Antarctic: Renewed potential for the application of GDGT-paleothermometry in lakes. Geochim. Cosmochim. Acta 75, 6225–6238. doi:10.1016/j.gca.2011.07.042

Pollard, D., DeConto, R.M., 2009. Modelling West Antarctic ice sheet growth and collapse through the past five million years. Nature 458, 329–332. doi:10.1038/nature07809

Russon, T., Elliot, M., Sadekov, A., Cabioch, G., Corrège, T., De Deckker, P., 2011. The mid-Pleistocene transition in the subtropical southwest Pacific. Paleoceanography 26. doi:10.1029/2010PA002019

Scherer, R.P., Bohaty, S.M., Dunbar, R.B., Esper, O., Flores, J.-A., Gersonde, R., Harwood, D.M., Roberts, A.P., Taviani, M., 2008. Antarctic records of precession-paced insolation-driven warming during early Pleistocene Marine Isotope Stage 31. Geophys. Res. Lett. 35. doi:10.1029/2007GL032254

Schouten, S., Huguet, C., Hopmans, E.C., Kienhuis, M.V.M., Sinninghe Damsté, J.S., 2007. Analytical Methodology for TEX_{86} Paleothermometry by High-Performance Liquid Chromatography/Atmospheric Pressure Chemical Ionization-Mass Spectrometry. Anal. Chem. 79, 2940–2944. doi:10.1021/ac062339v

Shanahan, T.M., Hughen, K.A., Van Mooy, B.A.S., 2013. Temperature sensitivity of branched and isoprenoid GDGTs in Arctic lakes. Org. Geochem. 64, 119–128. doi:10.1016/j.orggeochem.2013.09.010

Stocker, T.F., Qin, D., Plattner, G.-K., Tignor, M., Allen, S.K., Boschung, J., Nauels, A., Xia, Y., Bex, V., Midgley, P.M., 2013. Climate change 2013: The physical science basis. Intergov. Panel Clim. Change Work. Group Contrib. IPCC Fifth Assess. Rep. AR5Cambridge Univ Press N. Y.

Sun, Q., Chu, G., Liu, M., Xie, M., Li, S., Ling, Y., Wang, X., Shi, L., Jia, G., Lü, H., 2011. Distributions and temperature dependence of branched glycerol dialkyl glycerol tetraethers in recent lacustrine sediments from China and Nepal. J. Geophys. Res. 116. doi:10.1029/2010JG001365

Sun, Y., An, Z., Clemens, S.C., Bloemendal, J., Vandenberghe, J., 2010. Seven million years of wind and precipitation variability on the Chinese Loess Plateau. Earth Planet. Sci. Lett. 297, 525–535. doi:10.1016/j.epsl.2010.07.004

Teitler, L., Florindo, F., Warnke, D.A., Filippelli, G.M., Kupp, G., Taylor, B., 2015. Antarctic Ice Sheet response to a long warm interval across Marine Isotope Stage 31: A cross-latitudinal study of iceberg-rafted debris. Earth Planet. Sci. Lett. 409, 109–119. doi:10.1016/j.epsl.2014.10.037

Tierney, J.E., Russell, J.M., Eggermont, H., Hopmans, E.C., Verschuren, D., Sinninghe Damsté, J.S., 2010. Environmental controls on branched tetraether lipid distributions in tropical East African lake sediments. Geochim. Cosmochim. Acta 74, 4902–4918. doi:10.1016/j.gca.2010.06.002

Tripati, A.K., Roberts, C.D., Eagle, R.A., Li, G., 2011. A 20 million year record of planktic foraminiferal B/Ca ratios: Systematics and uncertainties in< i> p CO< sub> 2 reconstructions. Geochim. Cosmochim. Acta 75, 2582–2610.

Villa, G., Lupi, C., Cobianchi, M., Florindo, F., Pekar, S.F., 2008. A Pleistocene warming event at 1 Ma in Prydz Bay, East Antarctica: Evidence from ODP Site 1165. Palaeogeogr. Palaeoclimatol. Palaeoecol. 260, 230–244. doi:10.1016/j.palaeo.2007.08.017

Villa, G., Persico, D., Wise, S.W., Gadaleta, A., 2012. Calcareous nannofossil evidence for Marine Isotope Stage 31 (1Ma) in Core AND-1B, ANDRILL McMurdo Ice Shelf Project (Antarctica). Glob. Planet. Change 96-97, 75–86. doi:10.1016/j.gloplacha.2009.12.003

Weijers, J.W.H., Schouten, S., van den Donker, J.C., Hopmans, E.C., Sinninghe Damsté, J.S., 2007. Environmental controls on bacterial tetraether membrane lipid distribution in soils. Geochim. Cosmochim. Acta 71, 703–713. doi:10.1016/j.gca.2006.10.003

Yang, H., Pancost, R.D., Dang, X., Zhou, X., Evershed, R.P., Xiao, G., Tang, C., Gao, L., Guo, Z., Xie, S., 2014. Correlations between microbial tetraether lipids and environmental variables in Chinese soils: Optimizing the paleo-reconstructions in semi-arid and arid regions. Geochim. Cosmochim. Acta 126, 49–69. doi:10.1016/j.gca.2013.10.041

Figure Captions:

Figure 1: Approximate location of Lake El'gygytgyn in NE Siberia and other locations relevant to this study. Background image source: NASA's Earth Observatory.

Figure 2: brGDGT results from MIS 35-29 at Lake El'gygytgyn: a) concentrations of total brGDGTs relative to grams sediment extracted; b) MBT, c) CBT, and d) pH values calculated using equation of Weijers et al., (2007); e) MBT/CBT based temperatures calculated using equation of Sun et al. (2011). Pink shading denotes period from start of MIS 33 (1114 kyr BP) to end of MIS 31 (1062 kyr BP), dashed lines denote duration of MIS 31.

Figure 3: Compilation of proxy data from Lake El'gygytgyn: a) age model tie points from Nowaczyk et al. (2013), large black diamond represents 1st order paleomagnetic reversal, dark blue circles represent 2nd and 3rd order proxy tie points; b) brGDGT based temperatures (blue) (this study); pollen based mean temperature of the warmest month (MTWM) estimates (purple) (Melles et al., 2012); c) % tree and shrub pollen at the lake (green) (Melles et al., 2012); d) ratio of silica to titanium (Si/Ti) (gray), interpreted as a proxy for primary productivity. e) Red bars in bottom panel denote presence of interglacial (red) or super interglacial (dark red) facies (Melles et al., 2012). Long dashed line at 10ºC indicates modern mean July temperature. Maximum brGDGT temperature estimates from other Pleistocene interglacials indicated with shorter dashed lines (data from Brigham-Grette and Nolan, 2007; Habicht et al., in prep; Castañeda et al., in prep). Light pink shading denotes entire period from MIS 33-31 (1114-1062 kyr BP), darker pink shading denotes tranditional definition of MIS 31 (1082-1062 kyr BP) (Lisiecki and Raymo, 2005).

Figure 4: a) Lake El'gygytgyn age model tie points from Nowaczyk et al. (2013), large black diamond represents 1st order paleomagnetic reversal, dark blue circles indicate 2nd

and 3rd order proxy tie points; b) insolation values for 65°N (dashed red line) and 65°S (gray line) (Laskar et al., 2004); c) LR04 benthic stack (Lisiecki and Raymo, 2005); d) MBT/CBT temperature values from Lake El'gygytgyn (this study); e) and accumulation rate of IRD (ice-rafted detritus) from Site 1090 in South Atlantic (Teitler et al., 2015). Pink shading denotes period from start of MIS 33 (1114kyr BP) to end of MIS 31 (1062 kyr BP), dashed lines indicate traditional defintion of MIS 31 (1082-1062 kyr BP) (Lisiecki and Raymo, 2005).

Figure 5: Compilation of existing paleotemperature records of sufficient resolution to be relevant spanning MIS 31. Upper panel (Sites 772- 1123) depicts records where magnitude of cooling during MIS 32 appears reduced relative to other Early Pleistocene glacial periods: a) Site 772 (16°N, Herbert et al., 2010), b) Site 871 (5°N, Dyez et al., 2014), c) Site 847 (0°N, Medina-Elizalde et al., 2008), d) Site 849 (0°N, McClymont and Rosell-Melé, 2005), e) Site 846 (3°S, Herbert et al., 2010), f) Site MD06-301 (23°S, Russon et al., 2011), g) Site 1123 (41°S, Crundwell et al., 2008). Middle panel depicts h) biomarker based temperatures from Lake El'gygytgyn (this study) and i) the LR04 benthic stack (Lisiecki and Raymo, 2005) along with labels denoting marine isotope stages. Lower panel shows locations (Sites 306-1090) where, while cold "glacial" temperatures are recorded during MIS 32, the duration of cooling during appears abbreviated: j) Site 306-U1313 (41°N, Naafs et al., 2013), k) Site 1146 (19°N, Herbert et al., 2010), l) Site 1143 (9°N, Li et al., 2011), m) Site 1087 (31°S, McClymont et al., 2005b), n) Site 1090 (42°S, Martinez-Garcia et al., 2010). Pink shading denotes period from start of MIS 33 (1114kyr BP) to end of MIS 31 (1062 kyr BP), dashed lines indicate traditional defintion of MIS 31 (1082-1062 kyr BP) (Lisiecki and Raymo, 2005).

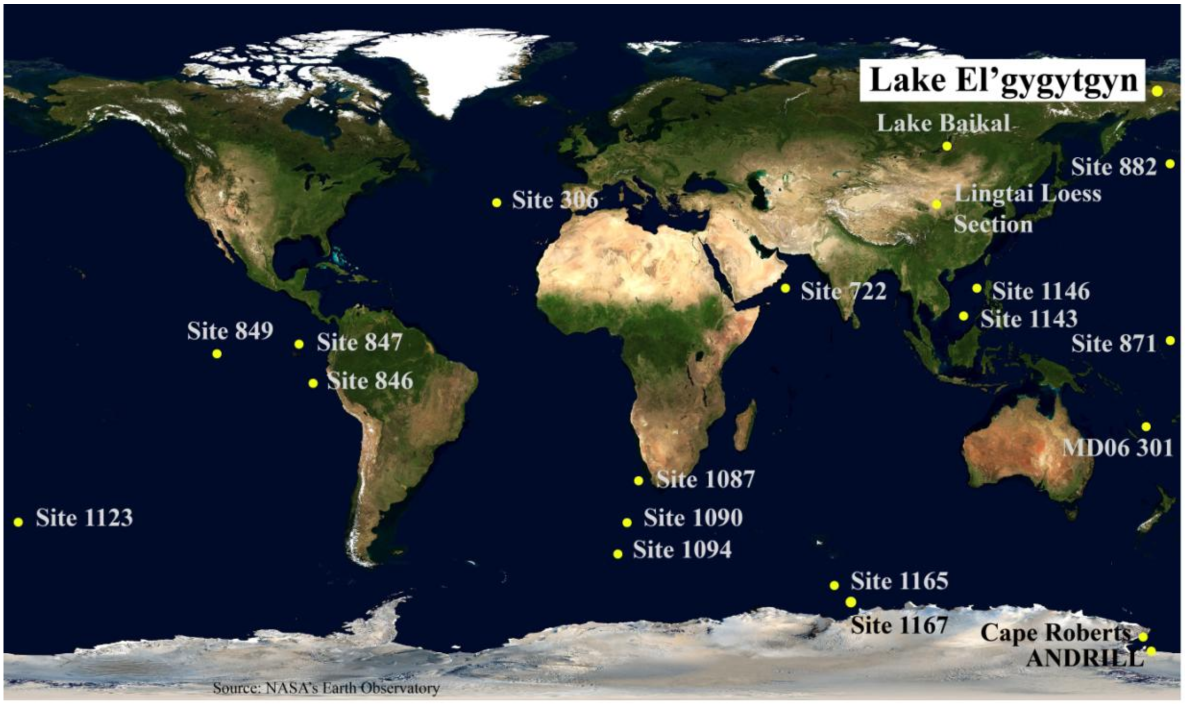
Lake El'gygytgyn
Lake Baikal
Site 882
Site 306
Lingtai Loess
Section
Site 722
Site 1146
Site 1143
Site 871
Site 849
Site 847
Site 846
MD06 301
Site 1087
Site 1123
Site 1090
Site 1094
Site 1165
Site 1167
Cape Roberts
ANDRILL
Source: NASA's Earth Observatory

Figure 1

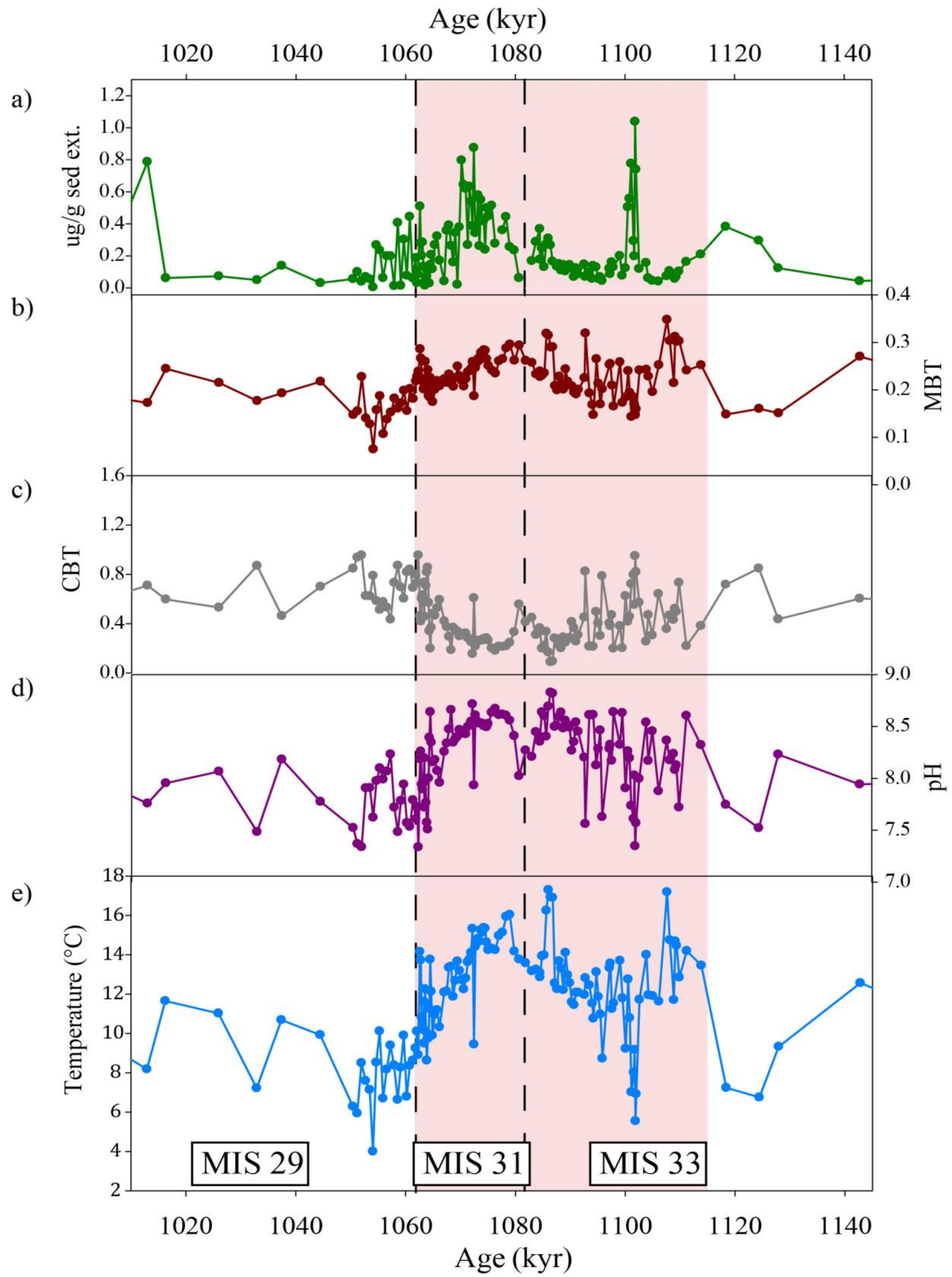
Age (kyr)
1020
1040
1060
1080
1100
1120
1140
a)
ug/g sed ext.
b)
MBT
c)
CBT
d)
pH
e)
Temperature (°C)
MIS 29
MIS 31
MIS 33
Age (kyr)

Figure 2

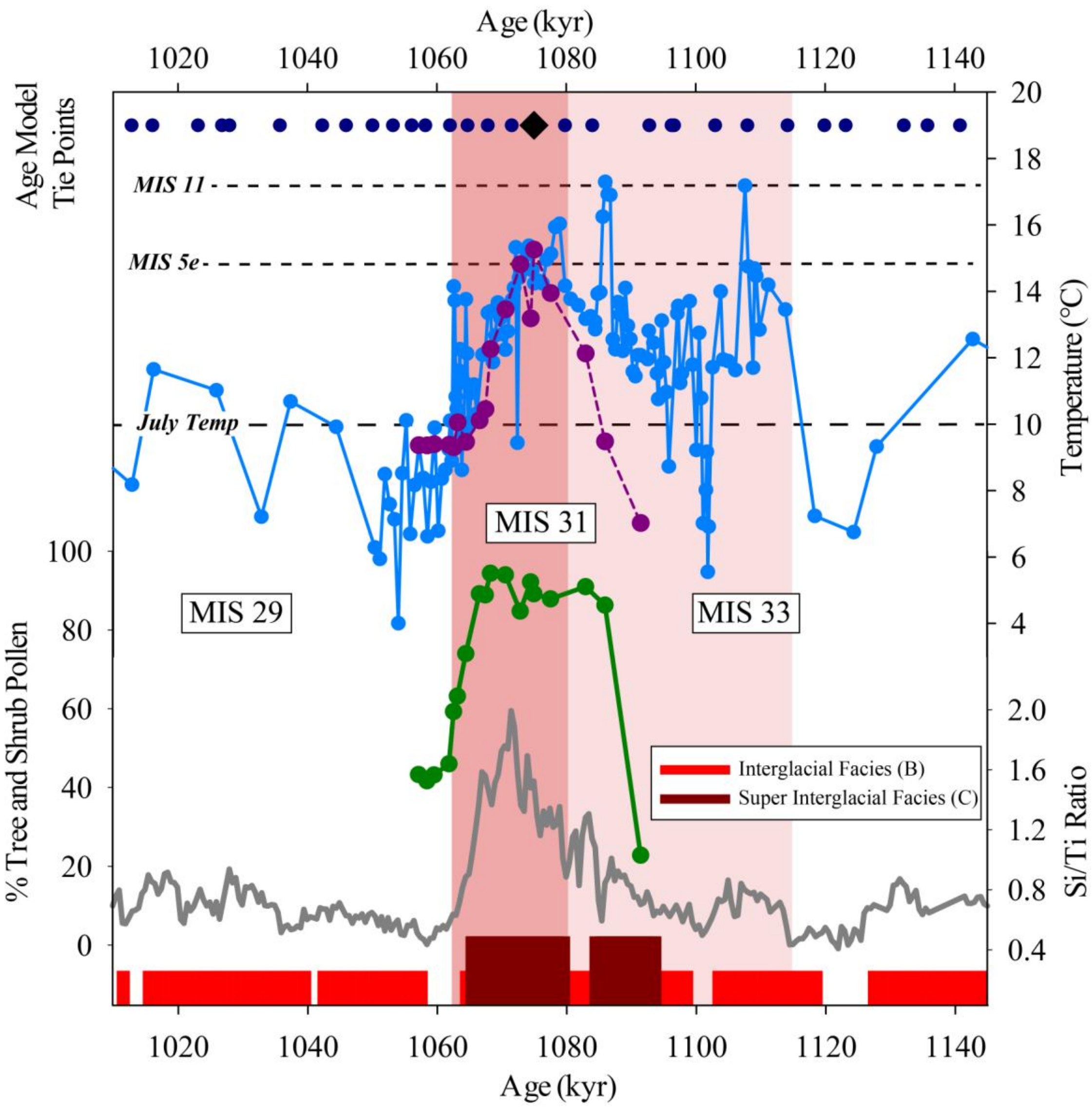

623
624 **Figure 3**

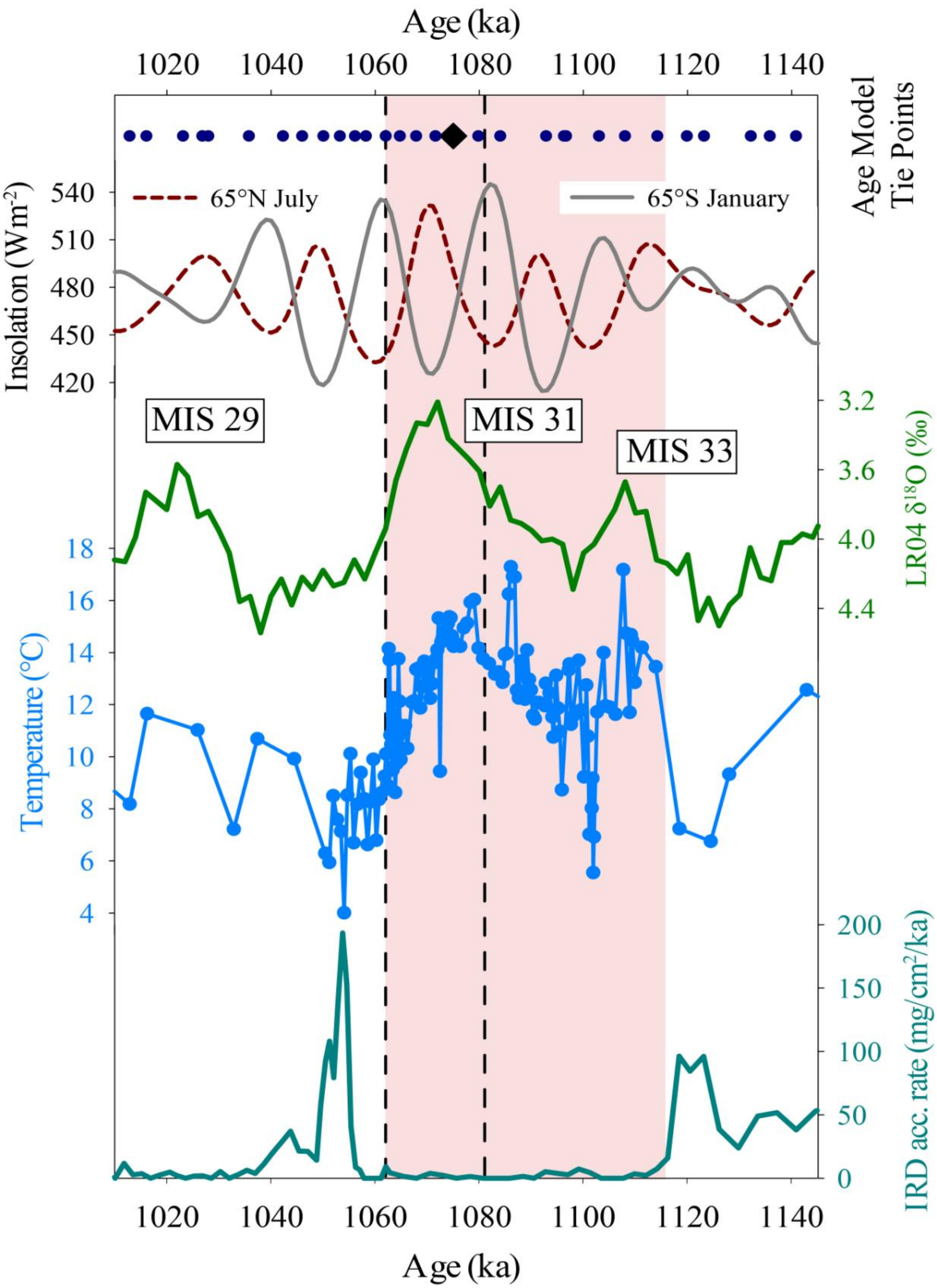
Age (ka)
1020 1040 1060 1080 1100 1120 1140
a)
Age Model
Tie Points
b)
Insolation (Wm-2)
540
510
480
450
420
65°N July
65°S January
MIS 29
MIS 31
MIS 33
c)
3.2
3.6
4.0
4.4
LR04 δ18O (‰)
d)
Temperature (°C)
18
16
14
12
10
8
6
4
e)
IRD acc. rate (mg/cm2/ka)
200
150
100
50
0
1020 1040 1060 1080 1100 1120 1140
Age (ka)

Figure 4

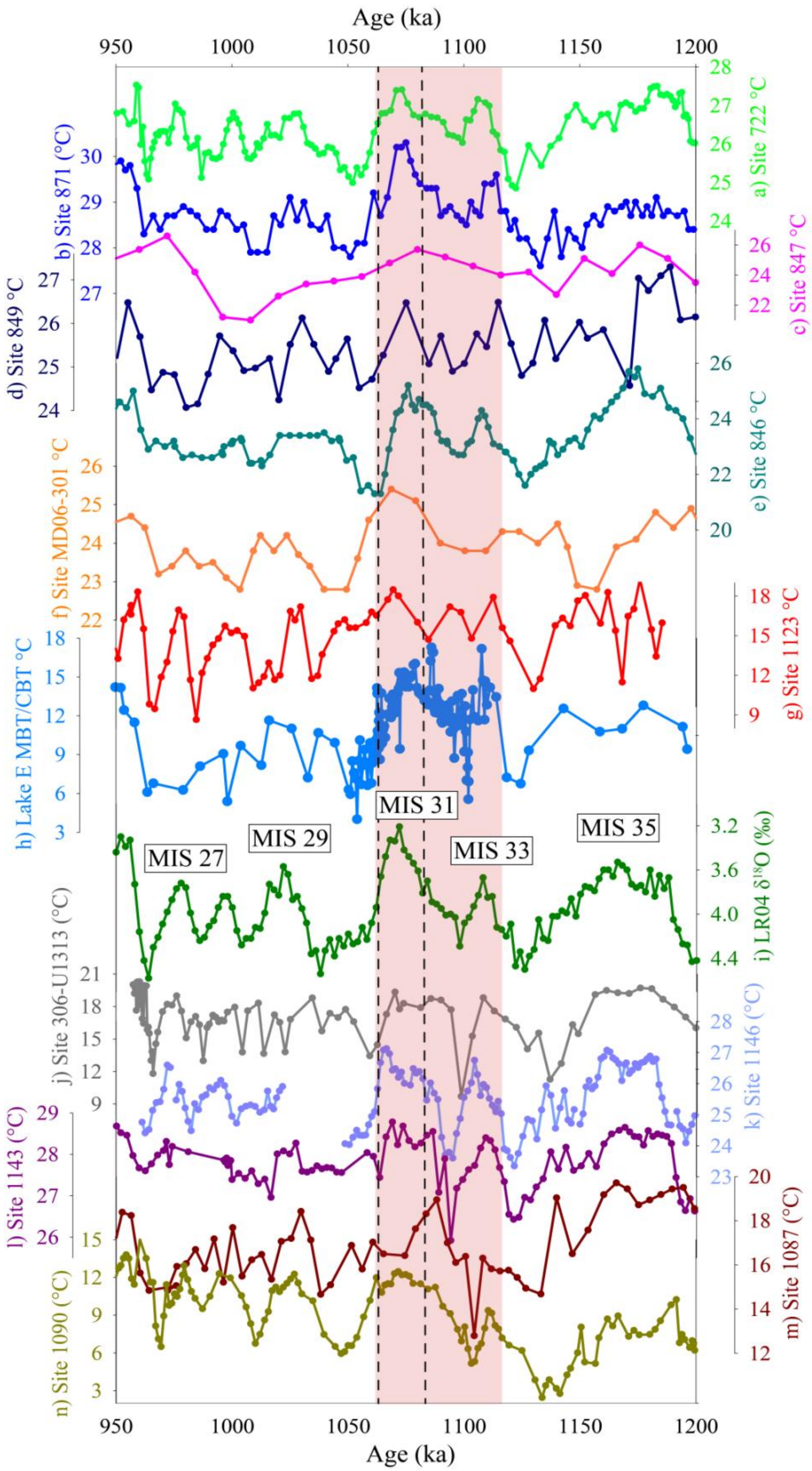
Age (ka)
950 1000 1050 1100 1150 1200
a) Site 722 °C
b) Site 871 (°C)
c) Site 847 °C
d) Site 849 °C
e) Site 846 °C
f) Site MD06-301 °C
g) Site 1123 °C
h) Lake E MBT/CBT °C
MIS 27
MIS 29
MIS 31
MIS 33
MIS 35
i) LR04 δ18O (‰)
j) Site 306-U1313 (°C)
k) Site 1146 (°C)
l) Site 1143 (°C)
m) Site 1087 (°C)
n) Site 1090 (°C)
Age (ka)

Figure 5